

**A STUDY OF A PLUNGING JET
BUBBLE COLUMN**

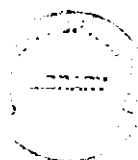
A thesis submitted for
the degree of
DOCTOR OF PHILOSOPHY

by

GEOFFREY MICHAEL EVANS

Department of Chemical Engineering
THE UNIVERSITY OF NEWCASTLE, N.S.W.

January, 1990



I hereby certify that the work
embodied in this thesis is the
result of original research and
has not been submitted for a
higher degree to any other
University or Institution.

(Signed) Geoffrey Evans

ACKNOWLEDGEMENTS

I am indebted to my supervisor Professor G.J. Jameson for his advice, suggestions and support throughout the course of this study, and for providing me with the opportunity to be involved in the industrial application of fundamental principles of fluid mechanics.

I wish to thank the technical and workshop staff of the Department of Chemical Engineering for their assistance, especially John Marsh and John Richards for their work in building the experimental apparatus, and Robin D'Ombrian and Bronwyn Middlebrook for their assistance with the photography and computing aspects of the project.

Special thanks are given to Mr. Neil Molloy of the Department of Mechanical Engineering for many enlightening discussions on the entrainment of plunging jets, and also to Dr. Chris Rielly of Cambridge University, England for his advice on the expansion of confined submerged jets.

Finally, my deepest appreciation to my wife, Jennifer, for the typing of the thesis, and also the patience and understanding she has shown throughout the period of this study.

ABSTRACT

The hydrodynamic phenomena occurring inside the enclosed downcomer section of a plunging jet bubble column are described in this study.

The gas entrainment rate for a plunging liquid jet was found to consist of two components, namely the gas trapped within the effective jet diameter at the point of impact, and the gas contained within the film between the jet and induction trumpet surface at the point of rupture. Entrainment within the effective jet diameter has been examined by McCarthy (1972). In this study, a model has been developed to predict the rate of filmwise entrainment. The model was supported by the experimental results, provided the film attained a region of constant thickness. When the induction trumpet was ruptured prior to a constant film thickness being reached, the measured rate of filmwise entrainment was higher than the prediction.

Filmwise entrainment was found to be initiated once a critical velocity along the surface of the induction trumpet was reached. The critical velocity was a function only of the liquid physical properties and was independent of the jet conditions and downcomer diameter. The velocity of the free surface of the induction trumpet was obtained from the velocity profile for the recirculating eddy generated by the confined plunging liquid jet.

The jet angle used to describe the expansion of the submerged jet inside the downcomer was predicted from the radial diffusion of jet momentum into the recirculating eddy. The model was able to predict the jet angle when it was assumed that the radial diffusion of jet momentum was a function of the Euler number based on the jet velocity and absolute pressure in the headspace at the top of the downcomer.

The model was also developed to predict the maximum stable bubble diameter generated within the submerged jet volume, where the energy dissipation attributed to bubble breakup was given by the energy mixing loss derived for the throat section of a liquid-jet-gas-pump. Good agreement was found between the measured and predicted maximum bubble

diameter values. The average experimental Sauter mean/maximum diameter ratio was found to be 0.61, which was similar to that for other bubble generation devices.

It was found that for turbulent liquid conditions in the uniform two-phase flow region, a transition from bubbly to churn-turbulent flow occurred at a gas void fraction of approximately 0.2 when the gas drift-flux was zero. Under laminar liquid flow, this transition took place at a gas void fraction above 0.3.

For the bubbly flow regime the Distribution parameter C_0 used by Zuber and Findlay (1965) to describe the velocity and gas void fraction profile, was found to be a function of the liquid Reynolds number. For laminar liquid flow, values of C_0 greater than unity were obtained. As the liquid Reynolds number was increased it was found that C_0 decreased, until a constant value of unity was obtained for fully turbulent flow.

For the churn-turbulent regime it was found that the gas void fraction measurements for all of the experimental runs could be collapsed onto a single curve when a modified gas void fraction was plotted against the gas-to-liquid volumetric flow ratio. The modified gas void fraction included a correction factor to account for the difference in the bubble slip velocity between the experimental runs. The experimental results also indicated that the value of the constant in the gas void fraction correction factor was different for laminar and turbulent flow.

Prior to bubble coalescence, it was found that the experimental drift-flux curves could be predicted from the measured bubble diameter, using the separated flow model developed by Ishii and Zuber (1979). After the onset of coalescence the drift flux measurements departed from the original drift-flux curves at a rate which increased linearly with increasing gas void fraction. It was found that the slope of the line fitted to the coalesced region of the drift-flux curves increased with increasing liquid Reynolds number and reached a constant value under fully turbulent flow conditions.

The model developed, together with the implications of the experimental results, are discussed with regard to optimising the design of an industrial plunging jet bubble column.

TABLE OF CONTENTS

	Page
ACKNOWLEDGEMENTS	i
ABSTRACT	ii
NOMENCLATURE	ix
 CHAPTER 1 INTRODUCTION	
1.1 Background to the study	1
1.2 Definition of problem	5
1.3 Research programme	6
1.4 Format of the thesis	10
 CHAPTER 2 BUBBLE COLUMNS: THEIR DESIGN AND HYDRODYNAMIC MODELLING	
2.1 Introduction	11
2.2 Types of gas-liquid contacting devices	12
2.3 Mechanically agitated reactor vessels	12
2.4 Reactor vessels without mechanical agitators	13
2.5 Bubble columns	
2.5.1 Reactor design	14
2.5.2 Hydrodynamic models	16
 CHAPTER 3 EXPERIMENTAL EQUIPMENT AND PROCEDURE	
3.1 Experimental programme	31
3.2 Materials	
3.2.1 Frother	32
3.2.2 Aqueous sucrose solution	33
3.2.3 Kerosene	34
3.3 Equipment	
3.3.1 Apparatus	35
3.3.2 Nozzle design	39
3.3.3 Column design	40
3.3.4 Pressure sensing equipment	41

	Page
3.4 Experimental procedure	
3.4.1 Jet diameter measurement	43
3.4.2 Jet length measurement	44
3.4.3 Gas void fraction measurement	44
3.4.4 Bubble diameter measurement	48
 CHAPTER 4 ENTRAINMENT BY A PLUNGING LIQUID JET	
4.1 Introduction	51
4.2 Literature review of plunging liquid jet systems	52
4.3 Modelling of confined jets	69
4.4 Theoretical development	
4.4.1 General description of the entrainment model	72
4.4.2 Calculation of the free-surface velocity of the induction trumpet	74
4.4.3 Calculation of entrained film volumetric flux	76
4.4.4 Prediction of the gas film thickness	81
4.5 Experimental description	83
4.6 Results and discussion	
4.6.1 Effect of free jet length on the gas entrainment rate	83
4.6.2 Effect of jet expansion on the gas entrainment rate	86
4.6.3 Determination of gas film entrainment rate	87
4.6.4 Effect of jet Weber number on the gas film component of the entrainment rate	88
4.6.5 Effect of column diameter on gas film entrainment	91
4.6.6 Effect of recirculating eddy velocity on the gas film thickness	95
4.6.7 Comparison of experimental and predicted gas film thickness values	98
4.6.8 Prediction of the initiation of gas film entrainment	100
4.7 Summary	106

	Page
CHAPTER 5 SUBMERGED JET EXPANSION AND BUBBLE GENERATION	
5.1 Introduction	107
5.2 Literature review	108
5.2.1 Critical bubble Weber number	109
5.2.2 Submerged liquid jet expansion	119
5.2.3 Bubble diameter distribution	122
5.3 Theoretical development	124
5.3.1 Expression for maximum bubble diameter	124
5.3.2 Specific energy dissipation rate for mixing zone	125
5.3.3 Estimation for mixing zone volume	128
5.4 Experimental	133
5.5 Results and discussion	134
5.5.1 Axial wall pressure measurements	134
5.5.2 Submerged jet angle	
(a) Effect of gas/liquid volumetric flow ratio	137
(b) Effect of column diameter	138
(c) Effect of liquid density	141
(d) Effect of jet diameter	143
(e) Effect of surface tension	144
(f) Effect of jet velocity	145
(g) Jet angle constant	147
5.5.3 Bubble diameter distribution	149
5.5.4 Maximum bubble diameter	151
(a) Effect of gas-to-liquid volumetric flow ratio	151
(b) Effect of column diameter	152
(c) Effect of kinematic viscosity	153
(d) Effect of jet velocity	154
(e) Effect of jet diameter	155
(f) Effect of surface tension	156
5.5.5 Bubble diameter ratio	157
5.6 Summary	157

	Page
CHAPTER 6	UNIFORM TWO-PHASE FLOW ZONE
6.1	Introduction 158
6.2	Single mixture models
6.2.1	One-dimensional drift-flux model 163
6.2.2	Two-dimensional drift-flux model 169
6.3	Separated flow model 173
6.4	Flow regime maps for cocurrent downward two-phase flow 179
6.5	Bubble coalescence 183
6.6	Transition from homogeneous to heterogeneous flow 188
6.7	Experimental description 190
6.8	Experimental results and discussion 190
6.8.1	Zuber and Findlay drift-flux plots 190
6.8.2	Bubbly flow regime
(a)	Distribution parameter 192
(b)	Bubble rise velocity 194
6.8.3	Transition from bubbly to churn-turbulent flow 196
6.8.4	Churn-turbulent flow
(a)	Distribution parameter 200
(b)	Bubble rise velocity 202
(c)	Gas void fraction 202
6.9	Summary 208
CHAPTER 7	OVERALL OPERATING CHARACTERISTICS
7.1	Introduction 210
7.2	Free jet 210
7.3	Plunging jet 212
7.4	Mixing zone 213
7.5	Uniform two-phase flow zone 215
7.6	Stability and operating ranges 216
CHAPTER 8	CONCLUSIONS AND RECOMMENDATIONS 217
REFERENCES	222

	Page
APPENDIX 1 SUMMARY OF CONDITIONS AND EXPERIMENTAL RESULTS	239
APPENDIX 2 PROPERTIES OF THE FREE JET	273
APPENDIX 3 BUBBLE SIZE MEASUREMENT	292
APPENDIX 4 AXIAL PRESSURE PROFILE AND SUBMERGED JET ANGLE MEASUREMENTS	298
APPENDIX 5 CALCULATIONS FOR CHAPTER 4	303
APPENDIX 6 PREDICTION OF SUBMERGED JET ANGLE	310

NOMENCLATURE

A	Area, (m^2)
b	Cross-sectional area ratio, (A_j/A_c)
C_0	Distribution parameter defined by (6.16)
D	Diameter, (m)
\mathcal{D}	Dispersion coefficient, (m^2s^{-1})
d	Diameter, (m)
E	Energy dissipation rate, (kgm^2s^{-3})
e	Energy dissipation, (kgm^2s^{-2})
F	Force, ($kgms^{-2}$)
f	Friction factor
G	Circulation strength, (s^{-1})
g	Acceleration due to gravity, (ms^{-2})
J	Total volumetric flux, (ms^{-1})
j	Volumetric flux (or superficial velocity), (ms^{-1})
k	Frictional loss coefficient
L	Length, (m)
M	Momentum, ($kgms^{-1}$)
N	Number
P	Pressure, ($kgms^{-2}$)
Q	Volumetric flowrate, (m^3s^{-1})
R	Radius, (m)
r	Radial co-ordinate, (m)
S	Surface roughness (defined in Figure 4.4), (m)
T	Film thickness, (m)
T_c	Film thickness in constant film thickness region, (m)
t	Time, (s)
V	Volume, (m^3)

V	Voltage, (volts)
v	Linear velocity, (ms^{-1})
W	Mass flowrate, (kgs^{-1})
y	Length from column wall, (m)
z	Axial length, (m)

GREEK SYMBOLS

β	Submerged jet angle, (degrees)
γ	Axis ratio, (length of maximum axis/length of minimum axis)
δ	Dirac delta function
ϵ	Gas void fraction
η	Energy transfer efficiency, (defined in 5.47)
θ	Nozzle contraction angle, (degrees)
χ	Film thickness ratio, (defined in 4.32)
μ	Absolute viscosity, ($\text{Pa}\cdot\text{s}$)
ν	Kinematic viscosity, (m^2s^{-1})
Ω	Packing parameter, (used in 6.50)
ρ	Density, (kgm^{-3})
σ	Surface tension, (Nm^{-1})
τ	Shear stress, ($\text{kgm}^{-1}\text{s}^{-2}$)
\varnothing	Angle of inclination from horizontal plane, (degrees)
ψ	Stream function
ω	Shear rate. (s^{-1})

SUPERSCRIPTS

*	Dimensionless quantity
'	Drift quantity

SUBSCRIPTS

B	Boundary layer
b	Bubble
c	Column
d	Droplet
e	Recirculating eddy
F	Film
f	Froth
G	Gas
I	Entrained gas component inside effective jet diameter
i	Interface
j	Jet
L	Liquid
M	Molecular
MZ	Mixing zone
m	Mean
N	Nozzle
o	Orifice
p	Pipe
r	Radial
S	Slip
s	Specific
T	Turbulent
VS	Volume-surface, or Sauter mean
w	Wall
z	Axial

DIMENSIONLESS NUMBERS

We	Weber number,	$\frac{\rho v^2 d}{\sigma}$.
Re	Reynolds number,	$\frac{\rho v d}{\mu}$.
Ca	Capillary number,	$\frac{\mu v}{\sigma}$.
N _H	Hill number,	$\frac{Q}{\sqrt{2\pi} r \sqrt{\frac{M}{\rho}}}$.
C _T	Crayner-Curtet number,	$\sqrt{\frac{2(N_H)^2}{1-(N_H)^2}}$.
Fr	Froude number,	$\frac{v^2}{gD}$.
Neu	Euler number,	$\frac{P_0}{\rho v^2}$.